

The Influence of Sodium Citrate and Potassium Sodium Tartrate Compound Additives on Copper Electrodeposition

Jiaqi Ni, Keqing Han^{*}, Muhuo Yu^{*}, Chenyu Zhang

State Key Laboratory for Modification of Chemical Fibers and Polymer Materials, College of Materials Science and Engineering, Donghua University, Shanghai 201620, P.R.China

^{*}E-mail: yumuhuo@dhu.edu.cn, hankeqing@dhu.edu.cn

Received: 4 April 2017 / *Accepted:* 12 May 2017 / *Published:* 12 June 2017

The effects of sodium citrate and potassium sodium tartrate as compound additives on copper electrodeposition from a sulfuric acid solution were investigated using different electrochemical measurements, including linear sweep voltammetry (LSV), cyclic voltammetry (CV), and chronoamperometry (CA). The LSV results revealed that the compound additives limited the hydrogen evolution reaction (HER) and impeded the reduction of copper ions on the surface of a vitreous carbon (VC) electrode. The CV results suggested that the deposition with or without additives was controlled by a diffusion-limited process. The real-time data of the current density vs. time obtained from CA implied that without the additives, the nucleation and growth mechanisms were relatively instantaneous three-dimensional (3D) diffusion controlled. Moreover, the presence of the compound additives did not change the mechanism. Their influence is that the additives absorbed on the electrode surface and/or complexed with the copper ions, inhibiting the reduction of the copper ions and reducing the rates of nucleation and growth.

Keywords: sodium citrate; potassium sodium tartrate; copper electrodeposition; nucleation and growth

1. INTRODUCTION

In recent decades, copper electrodeposition has been intensively researched, principally because of its wide variety of applications and developments in industries. Since 1997, electroplated copper has gradually replaced aluminum and plays a major role of as the metal for the interconnects in ultra large scale integrated circuits[1, 2]. Electroplated copper has also been adopted for use in the multilayer sandwiches of giant magneto resistive (GMR) hard disk read heads[3], active substrates for surface enhanced Raman spectroscopy[4], the formation of porous films as catalysts[5, 6], and in the preparation of I-III-V₂ semiconductors[7-9].

Traditionally, a cyanide bath was the most widely used technique for copper electroplating. However, due to its toxicity and harmfulness to the environment, the cyanide-based electrolyte has been undergoing replacement by non-cyanide formulations, for example, sulfate[10-12], chloride[13, 14], ammonia[15, 16] and pyrophosphate[17, 18].

Acid copper sulfate plating baths provide a number of desirable features. Their toxicity is fairly low, and they are environmentally friendly. They can operate at nearly 100% deposition efficiency and have a fast deposition rate. Additionally, the electroplated copper possesses great uniformity in both strength and ductility. As a result, acid copper sulfate baths have become the most widely used electrolyte for copper electrodeposition. It is well known that additives added to the plating bath will result in marked changes in the deposits. To effectively enhance the throwing power of plating baths, increase the current efficiency, and improve the quality of the deposits, which includes the brightness, hardness, smoothness and ductility, many kinds of additives are usually employed[3, 19-25].

The use of citrate and tartrate salts as additives in copper plating baths to improve the quality of electrodeposited copper has been widely reported [26-30]. Nevertheless, the effect of citrate and tartrate, as compound additives, on the process of copper electroplating, especially the nucleation and growth mechanism at the initial stage, has not yet been assessed to the best of our knowledge. Therefore, the objective of the present study is to investigate the effect of sodium potassium citrate and tartrate as compound additives on the initial stage of the copper electrodeposition process. For this purpose, different electrochemical methods were conducted to evaluate the influence of the compound additives on the electrochemical behaviors of copper electrodeposition.

2. EXPERIMENTAL

Experiments were performed in solutions containing copper sulfate as a copper ion source, and, potassium nitrate as a background electrolyte, with or without sodium citrate and sodium potassium tartrate as compound additives. The composition of the two main baths used for the electroplating of copper is presented in Table 1. All solutions used were prepared from analytical grade chemicals with double distilled water. The pH was adjusted to 4 using sulfuric acid or sodium carbonate.

The electrochemical experiments were conducted in a three-electrode cell, where either a vitreous carbon rod ($\varnothing=3$ mm), or a copper disk ($\varnothing=3$ mm) served as the working electrode (the disk was used for examining the behavior of the hydrogen evolution reaction (HER) on a copper base), a platinum sheet ($10\times 10\times 1$ mm³) served as the counter electrode, and an Ag/AgCl/KCl (3 M) electrode inserted into a Luggin capillary was used as a reference electrode to which all potentials in this paper are referred. Before every measurement, the working electrode was polished mechanically with 0.25 μm alumina powder in distilled water and then thoroughly rinsed with a nitric acid solution, ethanol, and distilled water under ultrasound, successively.

All the electrochemical experiments were conducted using a Zahner electrochemical workstation (Zennium/CIMPS-1) under computerized control. All the electrochemical measurements were performed at room temperature.

Table 1. Bath compositions for copper electrodeposition

Electrolytes	$\text{CuSO}_4 \cdot 5\text{H}_2\text{O}$ (M)	KNO_3 (M)	$\text{C}_6\text{H}_5\text{Na}_3\text{O}_7 \cdot 2\text{H}_2\text{O}$ (M)	$\text{C}_4\text{O}_6\text{H}_4\text{KNa} \cdot 4\text{H}_2\text{O}$ (M)	pH
(1)	0.2	0.18			4
(2)	0.2	0.18	0.35	0.05	4

3. RESULTS AND DISCUSSION

3.1. Linear sweep voltammetry

Fig. 1 shows the linear sweep voltammograms realized on a vitreous carbon (VC) electrode or a copper electrode in the different electrolyte solutions. Since there were no copper ions (the solid curves and dash curves in Fig. 1) in the electrolyte, only the HER and some complicated side reactions were observed. Without copper ions, on the VC electrode (the solid curves in Fig. 1), when there were no additives, the HER evolution occurred around -0.95 V. Conversely, with the additives, the HER evolution occurred at a more negative potential (approximately -1.08 V). The increase in the hydrogen overpotential and the decrease of the HER current density, especially at the high applied potentials, were due to the inhibitory effect of sodium citrate and sodium potassium tartrate compound additives on the HER. In addition, there is a small shoulder peak appearing at approximately -1.20 V in Fig. 1(a) and at approximately -1.30 V in Fig. 1(b). They may be associated with a complex nitrate reduction process, in which, nitrate ions may be reduced to NO_2^- , NO , N_2O , N_2 . Moreover, a noticeable reduction peak appeared near -1.48 V in Fig. 1(b). This may be a result of the reduction of the compound additives.

Without copper ions, on the copper electrode (the dash curves in Fig. 1), the HER appeared at approximately -0.7 V without additives, while it occurred at near -0.6 V with the compound additives added. Additionally, after adding the compound additives, the current density of the HER was increased. These changes are opposite to those that occurred on the VC electrode. This may be due to the inherent natures of the electrode materials. In addition, compared to the solid lines in Fig. 1, it can be easily concluded that the HER on the copper electrode is more liable to occur than on the VC electrode.

The dotted curves in Fig. 1 show the different results realized in solutions containing copper ions with a VC electrode. As seen, without the compound additives (Fig. 1(a)), the current density increased abruptly at the potential of 0.05 V, which was induced by the reduction of copper (I) ions and copper (II) ions. As the potential became more negative, a cathode current peak arises at approximately -0.13 V, which suggests a nucleation and growth mechanism that is controlled by diffusion[31]. While with the additives, the copper ion reduction potential shifted to a more negative value of approximately -0.14 V, and the cathode current peak subsequently appeared at approximately -0.25 V. As the potential shifts to more negative values, limiting current density regions became noteworthy. The limiting current density for a copper electrolyte without the additives was

approximately -18 mA cm^{-2} , while the values fell to -9.5 mA cm^{-2} when the additives were added, suggesting that the compound additives have a strong inhibitory effect on the reduction of copper ions on a VC electrode. The more negative peaks arising at approximately -0.80 V in both Fig. 1(a) and 1(b) may be associated with the redox reduction between metallic copper or copper (I) ions with nitrate ions in the acidic electrolytes.

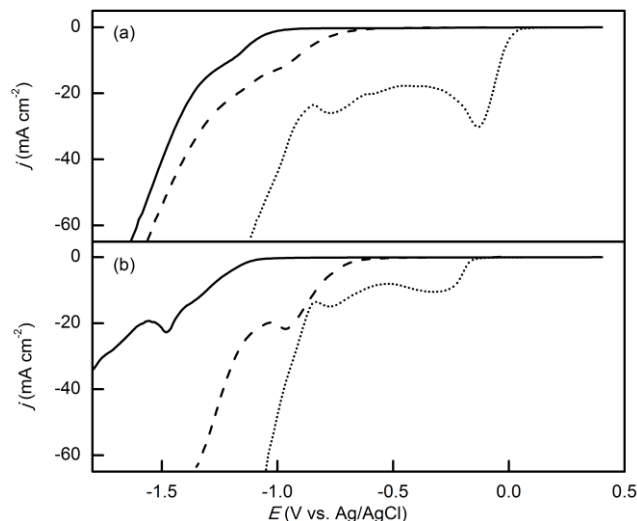


Figure 1. Linear sweep voltammograms obtained from solutions (a) without compound additives and (b) with compound additives ($0.35 \text{ M C}_6\text{H}_5\text{Na}_3\text{O}_7 \cdot 2\text{H}_2\text{O}$ and $0.5 \text{ M C}_4\text{O}_6\text{H}_4\text{KNa} \cdot 4\text{H}_2\text{O}$). Solid curves used a VC electrode and did not use Cu ions in the solution. Dotted curves used a VC electrode but did contain Cu ions in the solution. Dashed curves used a copper electrode and did not use Cu ions in the solution. Scan rate, 10 mV s^{-1} .

3.2 Cyclic voltammetry

The cyclic voltammograms recorded at various scan rates for copper electrodeposition in the absence and presence of the compound additives $\text{C}_6\text{H}_5\text{Na}_3\text{O}_7 \cdot 2\text{H}_2\text{O}$ and $\text{C}_4\text{O}_6\text{H}_4\text{KNa} \cdot 4\text{H}_2\text{O}$ are depicted in Fig. 2. In Fig. 2(a), the rapid increase in current density observed at approximately 0.25 V is assigned to the electroreduction of copper (II) ions at the cathode surface[32]. As the potential became more negative, the cathodic current density increased promptly, and a significant peak corresponding to copper crystallization appeared [32]. This is followed by a shoulder peak, which may be related to the electroreduction of copper (II) oxide or copper (I) oxide. After the peak, the voltammetric cathodic current decays and reaches to a limiting value which implies a mass transfer controlled process of the copper (I) ions and copper (II) ions electroreduction[33, 34]. By reversing the sweep, it is possible to note the cathodic current loop, typical of an overpotential-driven nucleation and growth electrodeposition process, and the characteristics associated with a nucleation followed by diffusion-limited growth process[32, 35]. In the positive branch, an anodic stripping peak is observed along with a small shoulder peak on the positive side of the peak. The stripping peak corresponds to the electrooxidation of metallic copper to copper (II) ions. The appearance of the shoulder peak

suggests that the comproportionation reaction between the copper (II) ions accumulating on the surface and the remainder of metallic copper occurs.

In Fig. 2(b), the trends of the cyclic voltammograms are similar to that in Fig. 2(a), but they have some differences. In the presence of the compound additives, the deposition potential shifted to a more negative value due to the strong inhibiting effect of the additives. It is also noted that the cathode current is decreased significantly in the presence of the compound additives, reaching approximately half of the value of Fig. 2(a) which is in a good agreement with the LSV results, suggesting the possibility of a complex formation in solution between the copper ion species and the additives[33]. Additionally, after adding the compound additives, the nucleation loops disappeared, which implies that the compound additives promoted the nucleation process and that there is no copper nucleus dissolved having a dimension that smaller than the critical nucleus radius. Finally, in the positive branch, there was only one stripping peak on each cyclic voltammogram, regardless of the scan rate. This implies that the compound additives have a strong chelating ability to free copper (II) ions and that the copper complex diffused to the bulk solutions quickly. In Fig. 2(a) and (b), the peak potential shifts negatively with the increase in the scan rate, suggesting the irreversibility of the reaction[36].

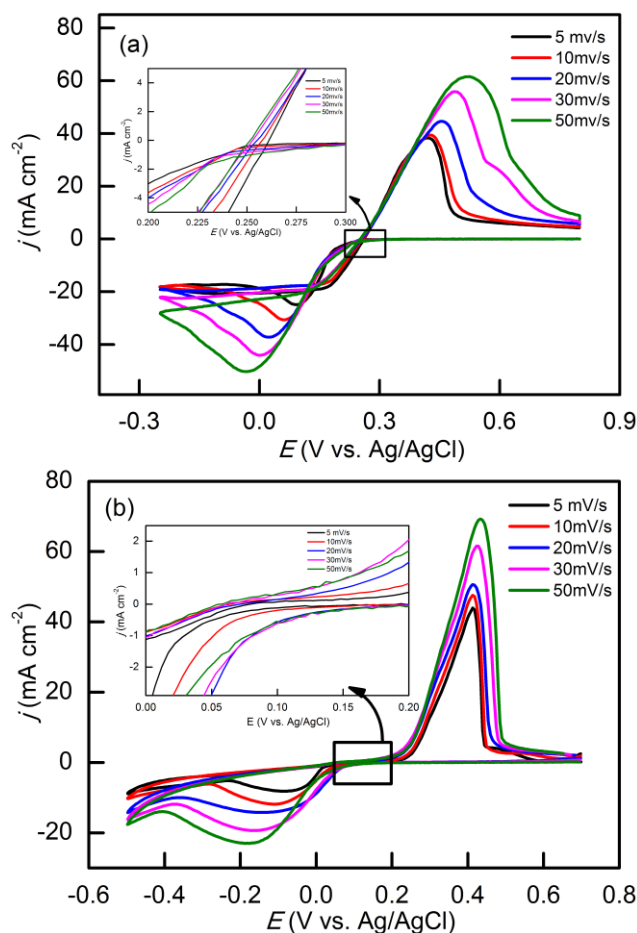


Figure 2. The cyclic voltammograms of copper electrodeposited on a vitreous carbon electrode from electrolytes without additives (a) and with additives (b) at different scan rates.

According to the Langmuir isothermal adsorption rule, there is a linear relationship between the cathodic peak current density (j_{pc}) and the square root of potential scan rates ($v^{1/2}$) if the current peak is caused only by ion diffusion. It can be seen from Fig. 3 that for both electrolytes systems, the relationship of j_{pc} and $v^{1/2}$ is linear, which implies that the mass transfer rate of copper ions transiting to the growing centers was the main control step of copper electrodeposition [35].

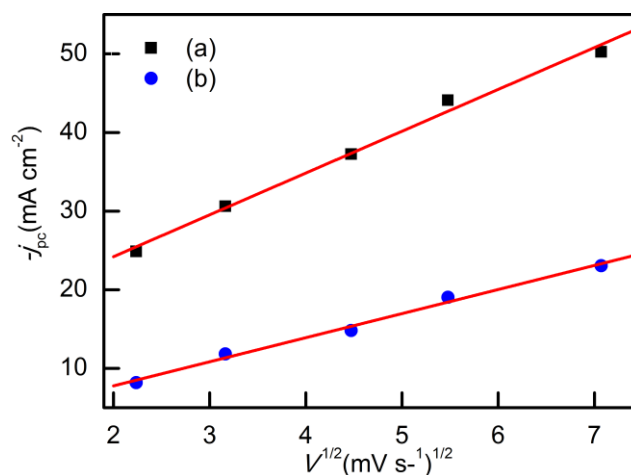


Figure 3. Linear relation between the cathodic peak current densities (j_{pc}) and the square root of potential scan rates ($V^{1/2}$) for electrolytes without additives (a) and with additives (b). The filled squares and circles represent the experimental data. The lines stand for the linear fit

3.3 Chronoamperometric curves

Electrochemical methods are considered to be better than other means of researching nucleation and growth because the nucleation's driving force can be changed simply by changing the potential applied [35]. In investigating the mechanism of the metal nucleation and growth process in greater detail, the method of analyzing current vs. time transients is regarded as quite useful and significant [35, 37]. The potentiostatic current transients presented in Fig. 4 were performed at a series of applied overpotentials in the absence and presence of the compound additives. The applied potential was stepped from 0.25 V to a potential set in the range 0 to -0.125 V. All the current transients showed the typical characteristics of an electrochemical nucleation and growth process [32, 34, 36]. Initially, charging the double layer resulted in a sharp decay in the current density within a very short time (as inserted graph clearly shows). Then, the cathodic current density increased up to a maximum, j_{max} , at t_{max} due to the copper crystal nucleation and growth on the VC electrode surface. Subsequently, the electroactive species linear diffusion to the planar surface contributed to a decaying current, which finally reached a constant value. The j_{max} increased while t_{max} decreased as the applied nucleation overpotential increased.

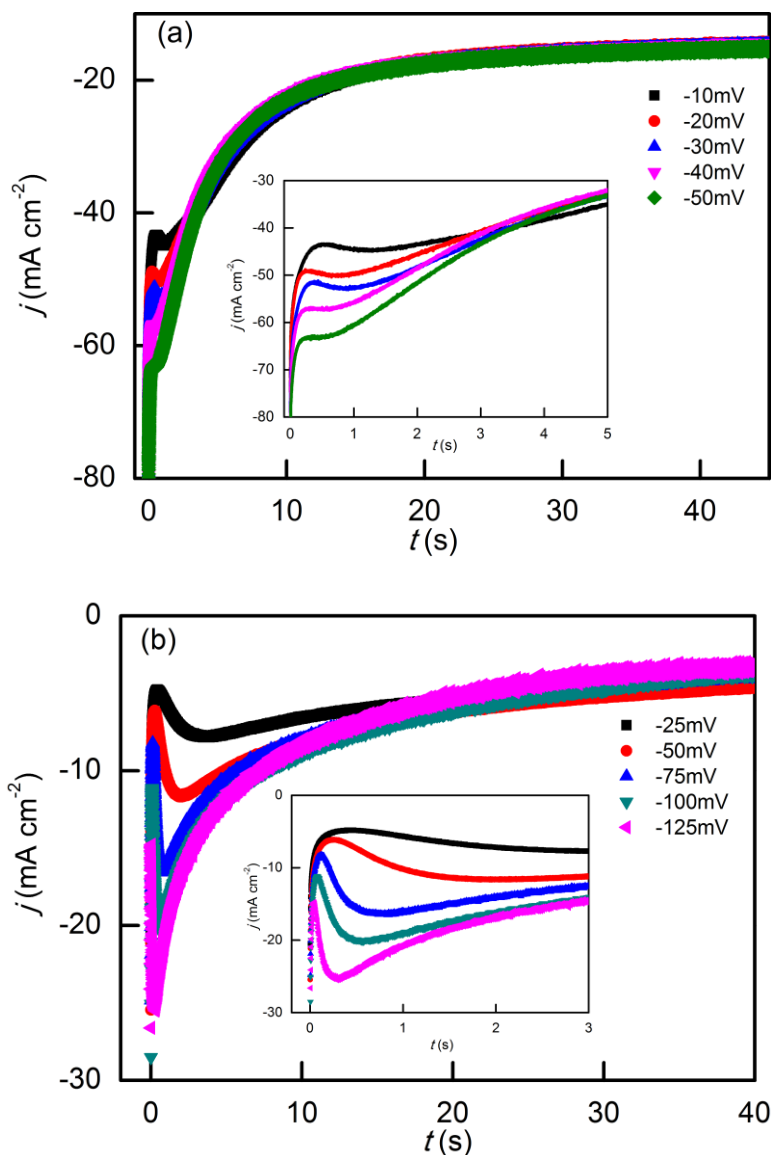


Figure 4. Current transients for copper deposition on vitreous carbon electrodes in electrolytes (a) without additives and (b) with the compound additives at different applied potentials.

Various theoretical models have been developed to describe the process of electrochemical nucleation. Of these, the Sharifker-Hills model, which is deduced from chronoamperometric experiments, has been identified as the most successful and has been used extensively [36, 38-41]. The model proposes two different limiting conditions: 3-D instantaneous and progressive nucleation[42]. The non-dimensional plots of $(j/j_{max})^2$ vs. (t/t_{max}) , play an important role in determining the nucleation behavior through comparison of the experimental results to the theoretical curves. For diffusion controlled 3-D instantaneous nucleation and growth[38, 39] ::

$$\frac{j^2}{j_{max}^2} = \frac{1.9542}{t/t_{max}} \{1 - \exp[-1.2564(\frac{t}{t_{max}})]\}^2 \quad (1)$$

and for progressive nucleation and growth [38, 39]:

$$\frac{j^2}{j_{max}^2} = \frac{1.2254}{t/t_{max}} \{1 - \exp[-2.3367(\frac{t}{t_{max}})^2]\}^2 \quad (2)$$

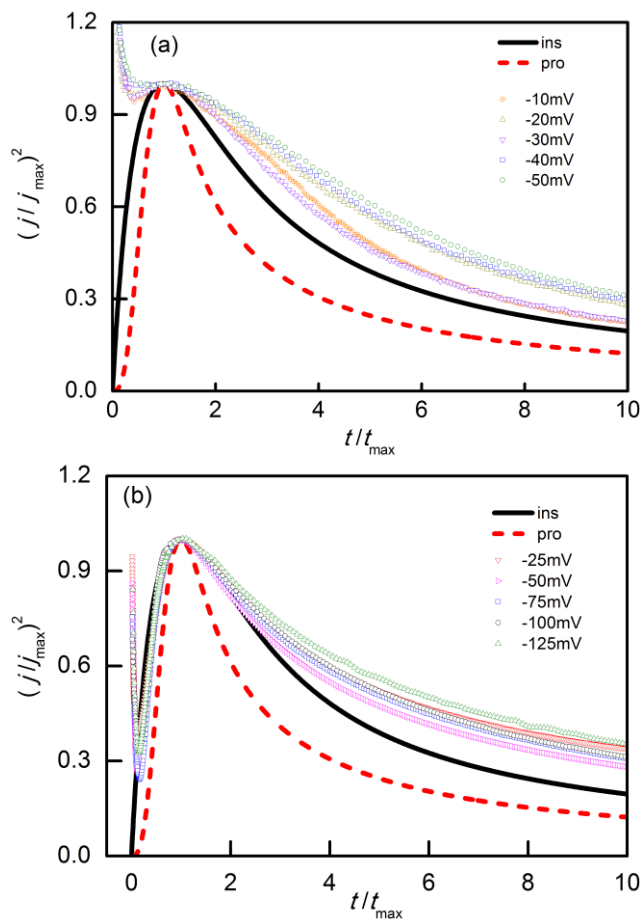
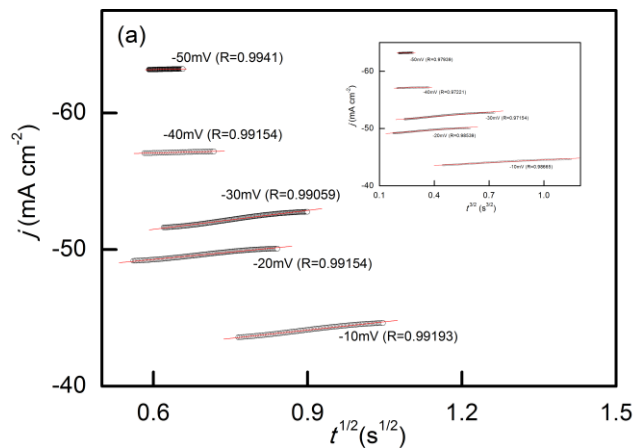


Figure 5. Normalized transients $(j/j_{max})^2$ vs. (t/t_{max}) curves of Figure 4. The solid black line represents the calculated curve for instantaneous nucleation, while the red dashed line represents progressive nucleation in each plot.

Fig. 5 presents the experimental normalized current-time transients compared to the theoretical transients calculated from Eqs. (1) and (2). It is found that without the additives, copper electrodeposition does not strictly follow either of the two nucleation mechanisms when the applied potential is in the range of -10 mV to -50 mV.



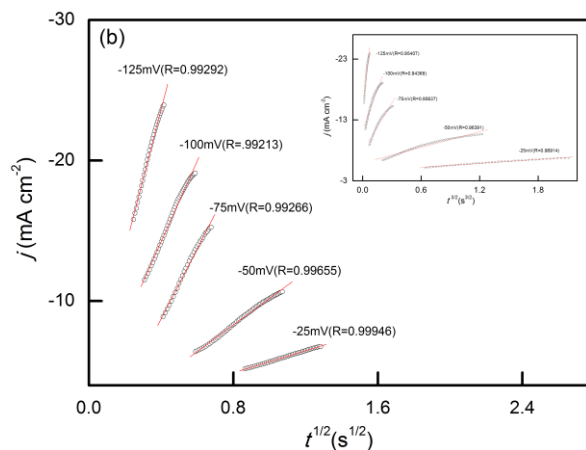


Figure 6. Dependence of j vs. $t^{1/2}$ plots for the initial transient portion of the curves from Figure 4 for copper depositing on vitreous carbon electrodes in electrolytes (a) without additives and (b) with the compound additives at different step potentials. The inserts show the same data for j vs. $t^{3/2}$ plots.

The curves in Fig. 5(b) are in considerable agreement with the instantaneous nucleation process when $t/t_{\max[2]} \leq 2$; however, the theoretical curve departs downward after $t/t_{\max} > 2$. The concomitant hydrogen evolution or the rapid replenishment of electroactive species through hemi-spherical diffusion to growth centers may contribute to the departure[43]. In addition, taking only the initial part into consideration, for the purpose of excluding the overlapping influence of growing 3D copper clusters and/or diffusions zones, the plots j vs. $t^{1/2}$ and j vs. $t^{2/3}$ (inset) are represented in Fig. 6. As it can be seen, linearity was improved for the j vs. $t^{1/2}$ plots, suggesting the occurrence of an instantaneous copper mode in the early nucleation process[35]. Nevertheless, in this model, deviations emerge after t_{\max} , which may be caused by a complex parallel response to the process of copper electrodeposition and the HER, which is favored on a previously electrodeposited copper cluster [44].

4. CONCLUSION

The influences of the compound additives, sodium citrate and potassium sodium tartrate, on copper electrodeposition were studied by different electrochemical techniques. Linear sweep voltammetry and cyclic voltammetry measurements show that the compound additives could lead to a higher overpotential for hydrogen evolution and could inhibit the hydrogen evolution reaction rate on a vitreous carbon electrode while promoting the rate on a copper electrode. Furthermore, the compound additives noticeably inhibit the reduction of copper ions. After the addition of the, the cathode limited current density declined to approximately 50% of the value without the compound additives. The results of the CV and CA indicate that the copper deposition on the vitreous carbon electrode corresponds to 3D diffusion-controlled growth, no matter if the additives are added or not. Without additives, copper deposition on a vitreous carbon electrode followed instantaneous nucleation, but not

strictly. Conversely, with the compound additives, the deposition process clearly followed the instantaneous nucleation mechanism.

References

1. J. Reid, *Jpn. J. Appl. Phys.*, 40 (2001) 2650.
2. P. C. Andricacos, C. Uzoh, J. O. Dukovic, J. Horkans and H. Deligianni, *IBM J. Res. Dev.*, 42 (1998) 567.
3. D. Grujicic and B. Pesic, *Electrochim. Acta*, 47 (2002) 2901.
4. V. Halouzka, B. Halouzкова, D. Jirovsky, D. Hemzal, P. Ondra, E. Siranidi, A. G. Kontos, P. Falaras and J. Hrbac, *Talanta*, 165 (2017) 384.
5. I. Najdovski, P. R. Selvakannan and A. P. O'Mullane, *Rsc Advances*, 4 (2014) 7207.
6. J. Niu, X. Liu, K. Xia, L. Xu, Y. Xu, X. Fang and W. Lu, *Int. J. Electrochem. Sci.*, 10 (2015) 7331.
7. S. Kim, D. J. Choi, K. R. Yoon, K. H. Kim and S. K. Koh, *Thin Solid Films*, 311 (1997) 218.
8. J. Klaer, J. Bruns, R. Henninger, K. Siemer, R. Klenk, K. Ellmer and D. Bräuning, *Semicond. Sci. Tech.*, 13 (1998) 1456.
9. R. Schrebler, M. Merino, P. Cury, M. Romo, R. Córdova, H. Gómez and E. A. Dalchiele, *Thin Solid Films*, 388 (2001) 201.
10. S. Esfandiarpour, L. Boehme and J. T. Hastings, *Nanotechnology*, 28 (2017) 125301.
11. M. Guo, M. Liu, W. Zhao, Y. Xia, W. Huang and Z. Li, *Appl Surf Sci*, 353 (2015) 1277.
12. J. Crousier and I. Bimaghra, *Electrochim. Acta*, 34 (1989) 1205.
13. N. Touabi, S. Martinez and M. Bounoughaz, *International Journal of Electrochemical Science*, 10 (2015) 7227.
14. S.J. Song, S.R. Choi, J.G. Kim and H.G. Kim, *Int. J. Electrochem. Sci.*, 11 (2016) 10067.
15. R. Drissi-Daoudi, A. Irhzo and A. Darchen, *J Appl Electrochem*, 33 (2003) 339.
16. D. Grujicic and B. Pesic, *Electrochim. Acta*, 47 (2002) 2901.
17. L. F. Senna, S. L. Díaz and L. Sathler, *J Appl Electrochem*, 33 (2003) 1155.
18. M. Cerisier, K. Attenborough, J. Fransaeer, C.V. Haesendonck, J.P. Celis, *J. Electrochem. Soc.* 146(6) (1999) 2156-2162.
19. W. Shao, G. Pattanaik, G. Zangari, W. Shao and G. Zangari, *J. Electrochem. Soc.*, 154 (2007) D201.
20. S. A. El Rehim, S. Sayyah and M. El Deeb, *Appl. Surf. Sci.*, 165 (2000) 249.
21. G. Fabricius, K. Kontturi and G. Sundholm, *J Appl Electrochem*, 26 (1996) 1179.
22. T. P. Moffat, D. Wheeler and D. Josell, *J. Electrochem. Soc.*, 151 (2004) C262.
23. S. S. A. E. Rehim, S. M. Sayyah and M. M. E. Deeb, *Appl. Surf. Sci.*, 165 (2000) 249.
24. D. F. Suarez and F. A. Olson, *J. Appl. Electrochem.*, 22 (1992) 1002.
25. E. C. Muñoz, R. S. Schrebler, P. K. Cury, C. A. Suarez, R. A. Córdova, C. H. Gómez, R. E. Marotti and E. A. Dalchiele, *J. Phys. Chem. B.*, 110 (2006) 21109.
26. R. Krumm, B. Guel, C. Schmitz and G. Staikov, *Electrochim. Acta.*, 45 (2000) 3255.
27. C. Zhao, China. CN103184487-A, 03 Jul 2013.
28. C. Zhao, China. CN103184488-A, 03 Jul 2013.
29. Y. Qian, China. CN103898571-A, 02 Jul 2014.
30. J. Tang, China. CN105132972-A, 09 Dec 2015.
31. J. Torrent-Burgués, E. Gaus and F. Sanz, *J. Appl. Electrochem.*, 32 (2002) 225.
32. Q. B. Zhang, Y. X. Hua and R. Wang, *Science China Chemistry*, 56 (2013) 1586.
33. L. Bonou, M. Eyraud, R. Denoyel and Y. Massiani, *Electrochim Acta*, 47 (2003) 4139.
34. A.E. Bolzán, Electrodeposition of copper on glassy carbon electrodes in the presence of picolinic acid, *Electrochim. Acta* 113(4) (2013) 706-718.
35. M. R. Khelladi, L. Mentar, A. Azizi, A. Sahari and A. Kahoul, *Materials Chemistry & Physics*, 115 (2009) 385.

36. J. Zhang, A. Liu, X. Ren, J. Zhang, P. Yang and M. An, *Rsc Advances*, 4 (2014) 38012.
37. C. Ehlers, U. König, G. Staikov and J. W. Schultze, *Electrochim Acta*, 47 (2001) 379.
38. G. Hills, A. K. Pour and B. Scharifker, *Electrochim. Acta.*, 28 (1983) 891.
39. Southampton Electrochemistry Group, *Instrumental Methods in Electrochemistry*, Horwood Publishing, (2001), UK.
40. P. Sebastián, E. Torralba, E. Vallés, A. Molina and E. Gómez, *Electrochim Acta*, 164 (2015) 187.
41. A.L. Portela, M.L. Teijelo, G.I. Lacconi, Mechanism of copper electrodeposition in the presence of picolinic acid, *Electrochim. Acta* 51(16) (2006) 3261-3268.
42. B. Scharifker and G. Hills, *Electrochim Acta*, 28 (1983) 879.
43. S. Floate, M. Hyde and R. G. Compton, *J Electroanal Chem*, 523 (2002) 49.
44. M. Palomar-Pardavé, B. R. Scharifker, E. M. Arce and M. Romero-Romo, *Electrochim. Acta.*, 50 (2005) 4736.

© 2017 The Authors. Published by ESG (www.electrochemsci.org). This article is an open access article distributed under the terms and conditions of the Creative Commons Attribution license (<http://creativecommons.org/licenses/by/4.0/>).